ADAPTIVE ARRAY DETECTION ALGORITHMS WITH STEERING VECTOR MISMATCH

LIM Chin Heng, Elias Aboutanios and Bernard Mulgrew

Institute for Digital Communications
School of Engineering & Electronics, University of Edinburgh
Mayfield Road, Edinburgh EH9 3JL, United Kingdom
Telephone: +44 (0)131 6507454
Fax: +44 (0)131 6506554
Email: C.H.Lim@ed.ac.uk, E.Aboutanios@ed.ac.uk, B.Mulgrew@ed.ac.uk

ABSTRACT

The problem of signals detection with known templates in coloured Gaussian interference is especially relevant for radar applications. The optimum detector requires knowledge of the true interference covariance matrix, which is usually unknown. In practice, the matrix is estimated from target-free training data that must be statistically homogeneous with the test data. Traditional approaches, like the GLRT and AMF, require the availability of such training data. These conditions are normally not always satisfied, which degrades the detection performance. Recently, two single data set approaches that deal only with the test data, namely the GMLED and MLED were introduced. In this paper, we examine the performance of these detection algorithms and their reduced-dimension counterparts under steering vector mismatches. We investigate the cases where there is a mismatch in the spatial and temporal steering vectors.

1. INTRODUCTION

The detection of signals with known steering vectors in zero-mean coloured Gaussian interference is particularly relevant to the radar community. The work reported in this paper is primarily concerned with the application of space-time adaptive processing (STAP) to radar target detection in interference (clutter plus noise).

The signal model used is as follows: Consider a radar system utilizing an N_s-element array with inter-element spacing d. The radar transmits an M_t-pulse waveform in its coherent processing interval (CPI). The received data can then be partitioned in both space and time, by using a sliding window, into an $(N \times M)$ space-time snapshot $\mathbf{X}'$. This partitioning will result in $K_T = (N_s - N + 1)(M_t - M + 1)$ snapshot matrices being generated for processing.

The columns of these space-time snapshots are then stacked into inter-leaved column vectors $\mathbf{x}_k$ of size $(NM \times 1)$. The K_T columns are then arranged as the columns of the $(NM \times K_T)$ matrix $\mathbf{X}$. The signal model used is then:

$$\mathbf{X} = \alpha \mathbf{s}\mathbf{t}^T + \mathbf{N} \tag{1}$$

where both $\mathbf{s}$ and $\mathbf{t}$ are space-time vectors and α is a complex amplitude.

$\mathbf{N}$ is the $(NM \times K_T)$ zero-mean Gaussian clutter-plus-noise matrix with independent and identically distributed (iid) columns $\mathbf{n}_k \sim \mathcal{CN}(\mathbf{0}, \mathbf{C})$. The space-time clutter-plus-noise covariance matrix is defined as $\mathbf{C}$, where $\mathbf{C} = \mathbf{E}[\mathbf{N}\mathbf{N}^{\mathbf{H}}]$ and $\mathbf{E}[*]$ is the expectation operator. Generally, the detection problem is treated as a hypothesis test with the null and alternative hypotheses:

$$H_0 : \ \mathbf{X} = \mathbf{N} \tag{2}$$

$$H_1 : \mathbf{X} = \alpha \mathbf{s}\mathbf{t}^T + \mathbf{N} \tag{3}$$

The optimum processor weights are given as $\mathbf{w}_{opt} = \beta \mathbf{C}^{-1}\mathbf{s}$ in [1]. For a data snapshot $\mathbf{x}$, which can be any one columns of $\mathbf{X}$, the resulting filter output y is:

$$y = \mathbf{w}^H \mathbf{x} = \beta^* \mathbf{s}^H \mathbf{C}^{-1} \mathbf{x} \tag{4}$$

and β is a complex arbitrary constant. The optimum processor can be viewed as a whitening filter stage followed by a matched filter stage [2]. The filter output power, $Y = |y|^2$, is then compared to a threshold γ, for a certain probability of false alarm P_{fa}. The detection test becomes

$$Y \underset{H_0}{\overset{H_1}{\gtrless}} \gamma \tag{5}$$

For any signal detection algorithm, a highly desirable property is the constant false alarm rate (CFAR) property. By selecting a suitable value of β, the optimum processor can be made to possess the CFAR property. The CFAR matched filter (MF) is obtained by setting $\beta = \left(\mathbf{s}^H \mathbf{C}^{-1} \mathbf{s}\right)^{-\frac{1}{2}}$ in the hypothesis test of equation (5).

Traditional detection algorithms, such as the generalised likelihood ratio test (GLRT) [3] or the adaptive matched filter (AMF) [4], require target-free training data that must be homogeneous with the test data. They can also be known as the two data set (TDS) algorithms since they require a separate set of training data to estimate the noise covariance matrix.

To implement the detection test, an estimate of the interference covariance matrix, $\widehat{\mathbf{C}} = \frac{1}{K_t} \sum_{k=0}^{K_t} \mathbf{z}_k \mathbf{z}_k^H$, is obtained from the secondary data $\mathbf{z}_k$ of size K_t. These K_t snapshots are usually obtained from other range cells [5], thus making the algorithms vulnerable to heterogeneity problems and resulting in a degradation in detection performance [6]. Their respective detection statistics are:

$$Y_{GLRT} = \frac{|\mathbf{s}^H \widehat{\mathbf{C}}^{-1} \mathbf{g}|^2}{\mathbf{s}^H \widehat{\mathbf{C}}^{-1} \mathbf{s} \left(1 + \frac{1}{K_t} \mathbf{g}^H \widehat{\mathbf{C}}^{-1} \mathbf{g}\right)} \tag{6}$$

$$Y_{AMF} = \frac{|\mathbf{s}^H \widehat{\mathbf{C}}^{-1}\mathbf{g}|^2}{\mathbf{s}^H \widehat{\mathbf{C}}^{-1}\mathbf{s}} \tag{7}$$

where **g** is the sample mean vector

$$\mathbf{g} = \frac{1}{|\mathbf{t}|}\mathbf{X}\mathbf{t}^* = \frac{1}{|\mathbf{t}|}\sum_{k=1}^{K_T}\mathbf{x}_k\mathbf{t}^*(k) \tag{8}$$

Two alternative approaches, the generalised maximum likelihood estimation detector (GMLED) and maximum likelihood estimation detector (MLED) were proposed in [7]. They only require the set of test data and thus can be called the single data set (SDS) algorithms. The signal-to-noise ratio (SNR) loss performance under steering vector mismatch of these two algorithms were studied in [8]. They operate solely on the test data and therefore eliminate the heterogeneity problem. The respective detection statistics are

$$Y_{GMLED} = \frac{|\mathbf{s}^H \mathbf{Q}^{-1}\mathbf{g}|^2}{\mathbf{s}^H \mathbf{Q}^{-1}\mathbf{s}\,(1+\mathbf{g}^H \mathbf{Q}^{-1}\mathbf{g})} \tag{9}$$

$$Y_{MLED} = \frac{|\mathbf{s}^H \mathbf{Q}^{-1}\mathbf{g}|^2}{\mathbf{s}^H \mathbf{Q}^{-1}\mathbf{s}} \tag{10}$$

where

$$\mathbf{Q} = \sum_{k=1}^{K_T}\mathbf{x}_k\mathbf{x}_k^H - \mathbf{g}\mathbf{g}^H \tag{11}$$

The reduced-dimension counterparts of the four abovementioned detection algorithms were analysed in [9] and [10] and their detection statistics are as follows:

$$Y_{JDL-GMLED} = \frac{|\widetilde{\mathbf{s}}^H \widetilde{\mathbf{Q}}^{-1}\widetilde{\mathbf{g}}|^2}{\widetilde{\mathbf{s}}^H \widetilde{\mathbf{Q}}^{-1}\widetilde{\mathbf{s}}\left(1+\widetilde{\mathbf{g}}^H \widetilde{\mathbf{Q}}^{-1}\widetilde{\mathbf{g}}\right)} \tag{12}$$

$$Y_{JDL-MLED} = \frac{|\widetilde{\mathbf{s}}^H \widetilde{\mathbf{Q}}^{-1}\widetilde{\mathbf{g}}|^2}{\widetilde{\mathbf{s}}^H \widetilde{\mathbf{Q}}^{-1}\widetilde{\mathbf{s}}} \tag{13}$$

$$Y_{JDL-GLRT} = \frac{|\widetilde{\mathbf{s}}^H \widetilde{\widehat{\mathbf{C}}}^{-1}\widetilde{\mathbf{g}}|^2}{\widetilde{\mathbf{s}}^H \widetilde{\widehat{\mathbf{C}}}^{-1}\widetilde{\mathbf{s}}\left(1+\frac{1}{K_t}\widetilde{\mathbf{g}}^H \widetilde{\widehat{\mathbf{C}}}^{-1}\widetilde{\mathbf{g}}\right)} \tag{14}$$

$$Y_{JDL-AMF} = \frac{|\widetilde{\mathbf{s}}^H \widetilde{\widehat{\mathbf{C}}}^{-1}\widetilde{\mathbf{g}}|^2}{\widetilde{\mathbf{s}}^H \widetilde{\widehat{\mathbf{C}}}^{-1}\widetilde{\mathbf{s}}} \tag{15}$$

where the $\sim$ indicate the angle-Doppler quantities, transformed from the space-time domain by a two-dimensional (2-D) discrete Fourier transformation (DFT) for the joint-domain localized (JDL) algorithm. Thereafter the angle-Doppler data is grouped into a $(N_a \times M_d)$ localized processing region and adaptive processing is restricted to this region.

The reduced-dimension detectors reduce the required sample support, thus increasing the robustness against heterogeneity, as presented in [5] and [11]. They are particularly applicable to heterogeneous environments where the clutter homogeneity assumption does not hold or independent training data is not readily available. Even so, for the TDS detectors, the detection performance may still degrade significantly in heterogeneous environments. In this sense, the SDS detectors will not encounter the heterogeneity problem since the data is obtained from the test data set.

Another advantage of using the reduced-dimension detectors is the reduction in computational complexity, due to the inversion of a smaller-dimensional matrix of size $(N_a M_d \times N_a M_d)$ as compared to a matrix of size $(NM \times NM)$. This reduction in computational complexity, from order $O(NM)^3$ to $O(N_a M_d)^3$, becomes significant when the order of NM becomes large.

In this paper, we examine the performance of the various detection algorithms under steering vector mismatch by using the receiver operating curves. *It is assumed that there exists a set of independent training data* $\{\mathbf{z}_k\}_{k=1}^{K_t}$*, that is homogeneous with the test data. In addition, for the purpose of analysis, it is also assumed that although the test data snapshots are obtained using a sliding window, the columns of* $\mathbf{X}$ *are statistically independent.*

The contribution of this paper is to present the receiver operating curves of the various detectors to complement the SINR performance curves presented in [8] and to present the reduced-dimension detectors as a follow-on to the SDS algorithms presented in [7]. The paper is organised as follows: In Section 2, we discuss the effects of the three types of mismatches. The simulation results are shown in Section 3, with a brief conclusion in Section 4.

2. STEERING VECTOR MISMATCH

When the presence of the target signal is unknown, the test signal steering vector has to sweep through the whole range of Doppler and angle frequencies. There may be a mismatch between the test steering vector and target steering vector and this results in a degradation in the detection performance.

In this paper, we discuss the effects of three types of mismatch by using the receiver operating curves. The mismatches are namely: a mismatch in $\mathbf{s}$, a mismatch in $\mathbf{t}$ and a mismatch in both $\mathbf{s}$ and $\mathbf{t}$. The presentation of the analysis will follow closely to that in [8].

The general expressions for the probability of false alarm P_{fa} and probability of detection P_d are:

$$P_{fa}(\gamma) = \int_0^1 (1+\tau)^{-L} f_{\beta,L+1,nm-1}(\eta)d\eta \tag{16}$$

and

$$P_d = \int_0^1 h(\eta) f_{\beta,L+1,nm-1}(\eta)d\eta \tag{17}$$

where $f_{\beta,L+1,nm-1}(\eta)$ is the type I beta distribution,

$$h(\eta) = 1-(1+\tau)^{-L}\sum_{l=1}^{L}\binom{L}{l}\tau^l G_l\left(\frac{\lambda}{1+\tau}\right) \tag{18}$$

and

$$G_l(q) = e^{-q}\sum_{p=0}^{l-1}\frac{q^n}{p!} \tag{19}$$

with $n = N$, $m = M$, $\lambda = K_T NM\rho$ for the full-dimension detectors and $n = N_a$, $m = M_d$, $\lambda = K_T N_a M_d \rho$ for the reduced-dimension detectors respectively. The specific parameter values for each algorithm are summarised in Table 1. ρ is the SNR of the filter output y and η has a type I beta distribution with $(L+1)$ and nm degrees of freedom. A detailed discussion of ρ and η can be found in [7] and [10].

Table 1: Summary of the P_{fa} and P_d expressions

Algorithm	P_{fa}	P_d	L	τ
AMF	eq (16)	eq (17)	$K_t - NM + 1$	$\frac{1}{K_t}\eta\gamma$
GLRT	eq (16)	eq (17)	$K_t - NM + 1$	$\frac{\gamma}{K_t - \gamma}$
MLED	eq (16)	eq (17)	$K_T - NM$	$\eta\gamma$
GMLED	eq (16)	eq (17)	$K_T - NM$	$\frac{\gamma}{1-\gamma}$
JDL-AMF	eq (16)	eq (17)	$K_t - N_a M_d + 1$	$\frac{1}{K_t}\eta\gamma$
JDL-GLRT	eq (16)	eq (17)	$K_t - N_a M_d + 1$	$\frac{\gamma}{K_t - \gamma}$
JDL-MLED	eq (16)	eq (17)	$K_T - N_a M_d$	$\eta\gamma$
JDL-GMLED	eq (16)	eq (17)	$K_T - N_a M_d$	$\frac{\gamma}{1-\gamma}$

For the GLRT and AMF, the effects of the first mismatch were discussed in [4] and [12]. For the GMLED and MLED, the effects of the three mismatches on the SINR performance were presented in [8]. The difference between the TDS and SDS algorithms stems from the fact that the latter project the received data into the signal and noise subspaces based on $\mathbf{t}$. This maximum likelihood separation between the noise and signal estimates results in a greater loss for the SDS algorithms when there is a steering vector mismatch.

2.1 Mismatch in $\mathbf{s}$

The first mismatch is in the space-time vector $\mathbf{s}$. As seen in Section 1, this mismatch does not affect $\mathbf{g}$, $\widetilde{\mathbf{g}}$, $\mathbf{Q}$ or $\widetilde{\mathbf{Q}}$. Therefore, the extent of the losses for all the detection algorithms are similar.

2.2 Mismatch in $\mathbf{t}$

The second mismatch is in the space-time vector $\mathbf{t}$ used to combine the snapshots coherently. For the full-dimension and reduced-dimension TDS detection algorithms, this mismatch will only affect $\mathbf{g}$ and $\widetilde{\mathbf{g}}$ respectively. However, this mismatch results in an additional loss for the SDS algorithms since $\mathbf{t}$ is used to project the received data into the signal and noise subspaces. The noise covariance matrix $\mathbf{Q}$ or $\widetilde{\mathbf{Q}}$ is obtained from this noise subspace, as seen in equation (11).

Therefore, in addition to the loss in $\mathbf{g}$ and $\widetilde{\mathbf{g}}$, the signal leaks into the noise subspace and affects $\mathbf{Q}$ and $\widetilde{\mathbf{Q}}$. The filter is then biased and there is a degradation in the detection performance as some parts of the signal will be filtered out. For the TDS algorithms, the noise covariance matrix $\mathbf{C}$ or $\widetilde{\mathbf{C}}$ are obtained from an independent training set and are thus not affected by this additional loss.

2.3 Mismatch in both $\mathbf{s}$ and $\mathbf{t}$

When there is a mismatch in both $\mathbf{s}$ and $\mathbf{t}$, the total effects will be the sum of the effects due to the individual mismatch in $\mathbf{s}$ and $\mathbf{t}$.

3. SIMULATION RESULTS

The detection algorithms in this paper were implemented and simulated under the various scenarios of mismatch discussed. The receiver operating curves are used to illustrate the effects of the different mismatches. We show results for $N = 10$, $M = 1$ and $N_a = 3$ and $M_d = 1$. For the full-dimension and reduced-dimension detection algorithms, $K_T = K_t = 2N$ and $K_T = K_t = 2N_a$ respectively and a P_{fa} of 10^{-2} was used. The simulation results were averaged over 30 realisations (each consisting 40000 Monte Carlo runs of the interference matrix.

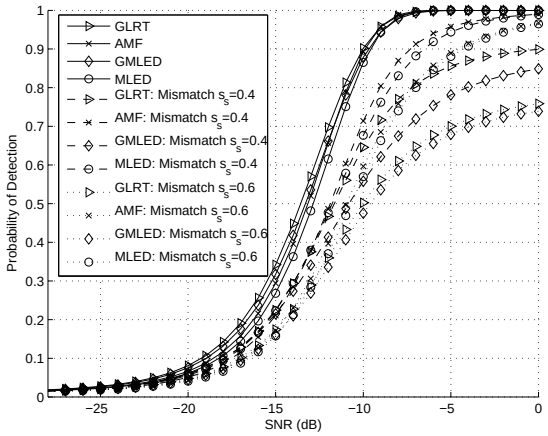

Figure 1: Probability of detection vs SNR for full-dimension detectors: $K_T = 20$ and $K_t = 20$ under mismatch in $\mathbf{s}$ of $\frac{0.4}{N}$ and $\frac{0.6}{N}$.

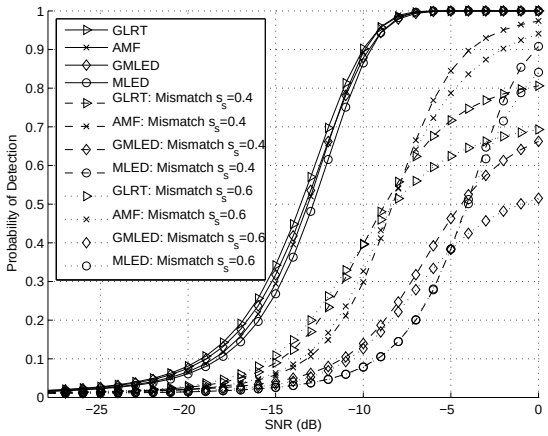

Figure 2: Probability of detection vs SNR for full-dimension detectors: $K_T = 20$ and $K_t = 20$ under mismatch in $\mathbf{s}$ of $\frac{0.4}{N}$ and $\frac{0.6}{N}$ when using non-iid snapshots.

The GLRT, AMF, GMLED and MLED, all with a known steering vector template, are given by the solid lines with triangles, crosses, diamonds and circles respectively. For the

reduced-dimension detectors, the same denotations are used. In all the figures, two sets of simulation results, in terms of the different mismatches of $\frac{0.4}{N}$ and $\frac{0.6}{N}$, are shown by the dashed and dotted lines.

Figures 1 and 2 show the effects on the detection performance, when the iid assumption of the snapshots are violated. It can be observed that when the iid assumption is not met, there is a general degradation for *all* the detectors in addition to the mismatch effect. At higher SNR, the generalised detectors (GLRT, GMLED, JDL-GLRT and JDL-GMLED) perform worse-off than the non-generalised detectors (AMF, MLED, JDL-AMF and JDL-MLED). It should be emphasised that the degradation is associated with *both* the SDS and TDS algorithms.

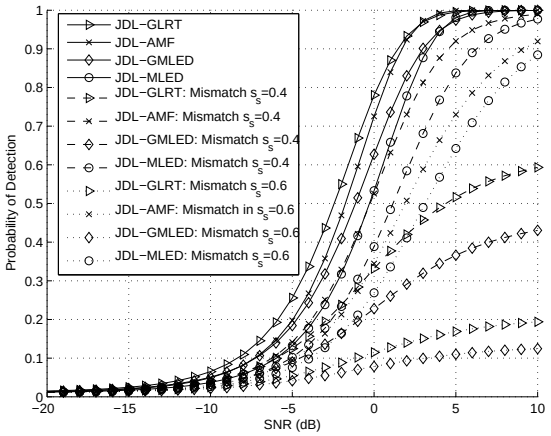

Figure 3: Probability of detection vs SNR for reduced-dimension detectors: $K_T = 6$ and $K_t = 6$ under mismatch in $\mathbf{s}$ of $\frac{0.4}{N}$ and $\frac{0.6}{N}$.

Figures 1 and 3 show the deterioration in detection performance when there is a mismatch in $\mathbf{s}$. As the magnitude of the mismatch is increased, the detection curves move to the right. The effects of the mismatch become more severe and eventually the P_d curves will tend to the P_{fa}.

From these two figures, it can be seen that the deterioration in the detection performance, caused by the mismatch, are more severe for the SDS algorithms. The extent of the deterioration effects are also greater for the reduced-dimension detectors than their full-dimension counterparts. Another important point to note is that, in each figure, the generalised detectors have a worse detection performance than the non-generalised detectors. This observation is consistent with what had been reported in [12].

Next, Figures 4 and 5 show the effects of a mismatch in $\mathbf{t}$. As mentioned in Section 2.2, the deterioration in the detection performance will be greater for the SDS detectors. This is due to the additional loss incurred from estimating the noise covariance matrix from the data.

As with the previous mismatch, the degradation effects are more severe for the reduced-dimension detectors (JDL-GLRT, JDL-AMF, JDL-GMLED and JDL-MLED). However, in this case, the generalised detectors perform better in the presence of a mismatch in $\mathbf{t}$.

The mismatch in $\mathbf{t}$ causes a greater degradation in the detection performance than the mismatch in $\mathbf{s}$. For the former, the detection curves tend faster to the P_{fa} when the absolute value of the mismatch is increased. This observation is consistent with what had been reported in [8].

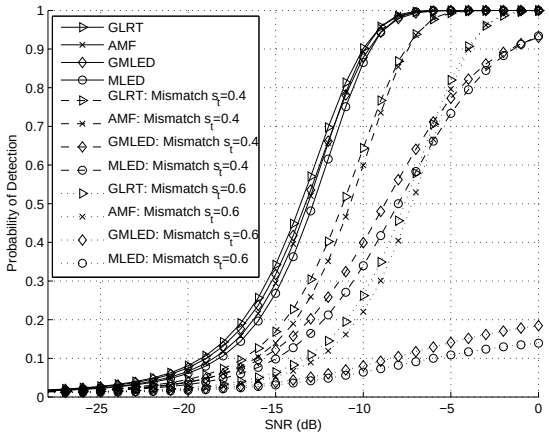

Figure 4: Probability of detection vs SNR for full-dimension detectors: $K_T = 20$ and $K_t = 20$ under mismatch in $\mathbf{t}$ of $\frac{0.4}{N}$ and $\frac{0.6}{N}$.

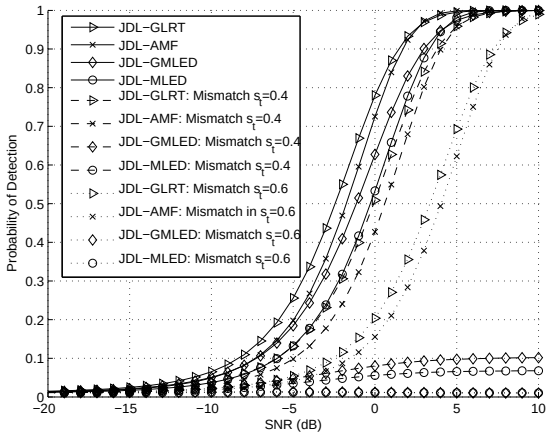

Figure 5: Probability of detection vs SNR for reduced-dimension detectors: $K_T = 6$ and $K_t = 6$ under mismatch in $\mathbf{t}$ of $\frac{0.4}{N}$ and $\frac{0.6}{N}$.

Finally, Figures 6 and 7 show the detection performance under both mismatches. The effects on the various detectors are a combination of the two mismatches. From Figure 6, it can be observed that the GMLED performs better than the MLED at low SNR. However, at high SNR, the opposite is true due to the effects of a mismatch in $\mathbf{s}$. There is a criss-crossing of the detection curves as the SNR increases. We note that the P_d curves tend to the P_{fa} when the mismatch is more severe in Figure 7. This observation can also be seen in Figure 5.

In summary, for the reduced-dimension detectors, the reduction in required sample support provides robustness

against heterogeneity and there is also a significant reduction in computational complexity. Although we had used $K_T = 6$ for the reduced-dimension SDS detectors in our simulations, more sample support can be used in heterogeneous environments since the SDS detectors will not be affected by the heterogeneity problems.

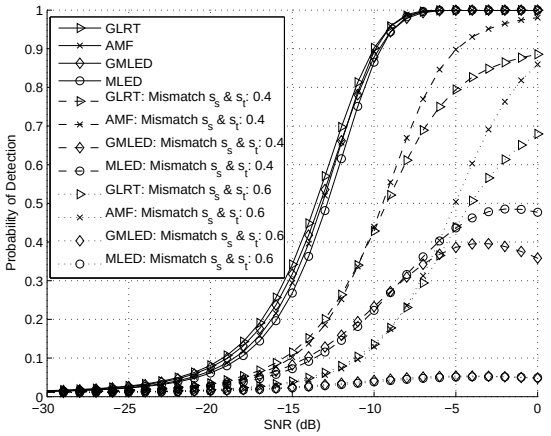

Figure 6: Probability of detection vs SNR for full-dimension detectors: $K_T = 20$ and $K_t = 20$ under mismatches in $\mathbf{s}$ and $\mathbf{t}$ of $\frac{0.4}{N}$ and $\frac{0.6}{N}$.

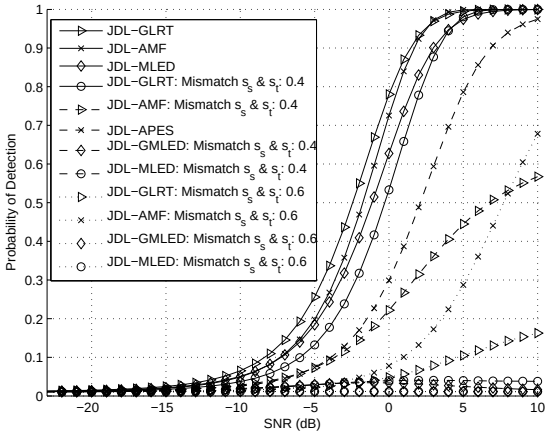

Figure 7: Probability of detection vs SNR for reduced-dimension detectors: $K_T = 6$ and $K_t = 6$ under mismatches in $\mathbf{s}$ and $\mathbf{t}$ of $\frac{0.2}{N}$ and $\frac{0.4}{N}$.

4. CONCLUSION

In this paper, we have examined the performance of the SDS and TDS detectors under steering vector mismatches. Three types of mismatches were discussed and the receiver operating curves were used to illustrate the effects of these mismatches. For the mismatch in $\mathbf{s}$, the observations were consistent with those reported in the current literature. As for the mismatch in $\mathbf{t}$, the SDS detectors were shown to suffer an additional loss from estimating the noise covariance matrix directly from the data. When there is a mismatch in both space-time vectors, the resulting effects are a combination of the individual mismatch in each vector. The reduced-dimension SDS detectors are particularly applicable to heterogeneous environments where the clutter homogeneity assumption deos not hold or independent training data is not readily available.

5. ACKNOWLEDGE

The authors would like to thank the support of BAE Systems and SELEX Sensors and Airborne Systems Ltd for this work.

REFERENCES

[1] L. Brennan and I. Reed, "Theory of adaptive radar," *IEEE Transactions on Aerospace and Electronic Systems*, vol. AES-9, no. 2, pp. 237–252, March 1973.

[2] R. Klemm, *Principles of space-time adaptive processing*. IEE Radar, Sonar, Navigation and Avionics Series, second edition, 2002.

[3] E. Kelly, "An adaptive detection algorithm," *IEEE Transactions on Aerospace and Electronic Systems*, vol. AES-22, no. 1, pp. 115–127, March 1986.

[4] F. Robey, D. Fuhrmann, K. E., and R. Nitzberg, "A CFAR adaptive matched filter detector," *IEEE Transactions on Aerospace and Electronic Systems*, vol. 28, no. 1, pp. 208–216, January 1992.

[5] J. Ward, "Space-time adaptive processing for airborne radar," MIT Lincoln Laboratory, Tech. Rep., 1994.

[6] M. Melvin, "Space-time adaptive radar performance in heterogeneous clutter," *IEEE Transactions on Aerospace and Electronic Systems*, vol. 36, pp. 621–633, April 2000.

[7] E. Aboutanios and B. Mulgrew, "A STAP algorithm for radar target detection in heterogeneous environments," *IEEE Workshop on Statistical Signal Processing*, July 2005.

[8] ——, "Assessment of the single data set detection algorithms under template mismatch," *IEEE International Symposium on Signal Processing and Information Technology*, December 2005.

[9] H. Wang and L. Cai, "On adaptive spatial-temporal processing for airborne radar systems," *IEEE Transactions on Aerospace and Electronic Systems*, vol. 30, no. 3, pp. 660–670, July 1994.

[10] C. Lim, E. Aboutanios, and B. Mulgrew, "Training strategies for JDL-STAP in a bistatic environment," *IEE Proceedings on Radar, Sonar and Navigation*, Accepted for publication.

[11] R. Adve, P. Antonik, W. Baldygo, C. Capraro, G. Capraro, T. Hale, R. Schneible, and M. Wicks, "Knowledge-base application to ground moving target detection," *Technical Report AFRL-SN-RS-TR-2001-185, Air Force Research Laboratory*, September 2001.

[12] S. Kalson, "An adaptive array detector with mismatched signal rejection," *IEEE Transactions on Aerospace and Electronic Systems*, vol. 28, no. 1, pp. 195–207, January 1992.